CBID: A Customer Behavior Identification System using Passive Tags

Jinsong Han*, Han Ding*, Chen Qian†, Dan Ma*, Wei Xi*, Zhi Wang*, Zhiping Jiang* and Longfei Shangguan‡
*School of Electronic and Information Engineering, Xi'an Jiaotong University, China
†Department of Computer Science, University of Kentucky, Lexington, Ky, USA
‡Hong Kong University of Science and Technology, Hong Kong
Email: {hanjinsong, zhiwang}@mail.xjtu.edu.cn, dinghan.331@stu.xjtu.edu.cn,
{madan.dan1019, weixi.cs, jiangzp.cs}@gmail.com, qian@cs.uky.edu, lshangguan@cse.ust.hk

***Abstract*—Different from online shopping, in-store shopping has few ways to collect the customer behaviors before purchase. In this paper, we present the design and implementation of an on-site Customer Behavior IDentification system based on passive RFID tags, named CBID. By collecting and analyzing wireless signal features, CBID can detect and track tag movements and further infer corresponding customer behaviors. We model three main objectives of behavior identification by concrete problems and solve them using novel protocols and algorithms. The design innovations of this work include a Doppler effect based protocol to detect tag movements, an accurate Doppler frequency estimation algorithm, a multi-RSS based tag localization protocol, and a tag clustering algorithm using cosine similarity. We have implemented a prototype of CBID in which all components are built by off-the-shelf devices. We have deployed CBID in real environments and conducted extensive experiments to demonstrate the accuracy and efficiency of CBID in customer behavior identification.**

I. Introduction

Customer shopping behavior analysis is of importance to improve retailer profits and customer experience. Compared to online shopping, in-store shopping such as Brick-and-Mortar (B&M) business lacks of effective approaches to identify comprehensive customer behaviors, such as picking up items, trying-on clothes, and price comparisons. Although mining of sales history has shown a success in telling customer behaviors [1], customer behaviors before the purchase, where rich information about shopping patterns exist, are not collected and analyzed. Therefore an on-site customer behavior identification system is highly desired by retailers to collect the data characterizing customer actions during the entire shopping procedure. Mining of such data could provide deep and comprehensive insights of customer interests, experiences, and expectations, which are important to improve service quality and profits of retailers. Ultimately, such a system would be a fundamental component for the emerging concept, Omni-channel Retailing, where customers should have a consistent and seamless experience in both in-store and online shopping [2].

Recent advances of the Radio Frequency Identification (RFID) technology provide new opportunities in building a cost-efficient item tracking and monitoring system [3][4][5][6]. Retailers can label items with low-cost and battery-free RFID tags (also known as passive tags). Compared to traditional Barcode labels, RFID tags can be remotely read in a non-line-of-sight manner, enabling automatic identification and processing [7][8]. It is reported that about 3 billion tags will be consumed by retailers in 2014 [9]. However, there is a major challenge for an RFID system to perform behavior identification. Since passive tags are originally designed for identity recognition only, their computing and memory resource is extremely limited. Hence passive tags are not able to report or compute their movements or locations, nor can they carry special devices such as accelerometer or GPS.

/978-1-4799-6204-4/14$31.00

In this work, we present the design, implementation, and evaluation of an RFID-based Customer Behavior IDentification system, named CBID. CBID is implemented by a commodity RFID reader and off-the-shelf tags. We have designed extensive protocols and algorithms to collect and analyze physical-layer data of the communication between the reader and passive tags. The data analysis identifies various human actions applied to tagged items.

Specifically, CBID focuses on performing three types of customer behavior analysis.

1) CBID enables item popularity discovery by counting the pick-up actions of the displayed items. We design a novel Doppler effect based movement detection protocol to count the pick-up actions applied to passive tags.

2) CBID is able to discover items with explicit correlations such as rival and complementarity. We model this task as detection of items that are held by a same customer. We design a new tag localization protocol based on the changes of radio signal strength. Tag locations allow CBID to determine the items that are likely to be held by a same person.

3) CBID helps to discover items that will be eventually selected by a same customer, although they are not directly rival or complementary. We call such relationships as implicit correlations and model this task as finding tags with a same movement trajectory. We design a moving tag clustering algorithm to accurately solve this problem in a short time duration.

We have successfully deployed CBID in various environments including a laboratory in a supermarket-like lay out and

a university library. Extensive experiments show that CBID achieves high accuracy of behavior identification.

We summarize our contributions in this work are as follows.

- To the best of our knowledge, we are the first to propose a passive tag based customer behavior identification system. We model three main objectives of behavior identification by concrete problems and solve them using wireless communication protocols and algorithms.
- We propose a new Doppler frequency based solution for detecting tag movements. We employ a phase-based Doppler frequency estimation method to overcome the problem of inaccurate measurements incurred by the current reader hardware.
- We propose a new metric, called Integration of Multi-RSS, for accurate tag localization. Our solution does not need hardware modifications on RFID devices.
- We develop a new moving tag clustering algorithm which is fast and accurate.
- We implement a prototype of CBID and conduct comprehensive experiments covering three major display styles in B&M stores. Experimental results show that CBID can achieve high accuracy of customer behavior identification in real environments.

II. Objectives and Overview

In this section, we present three main objectives of the CBID system. Then we introduce the signal characteristics we measured for customer behavior analysis and present an overview of CBID system design.

A. Objectives of CBID

The CBID system is designed to identify customer behaviors by collecting and analyzing wireless signal changes of RFID reader and tag communication. Specifically, CBID has three main objectives, namely discovering popular items, revealing explicit correlations, and disclosing implicit correlations.

1) ***Discovering popular items****: Popular items* are the ones with great interests of customers. Customer behavior analysis of sales history can only consider the purchase actions to indicate interests of items. The unique advantage of CBID is that it can identify other actions such as picking up an item, as shown in Figure 1(a). Intuitively, the more times an item is picked, the more attention the item gains. B&M stores can then adjust the display accordingly. In the CBID system, we count the detected pick-up actions of an item as a metric to reflect the amount of customer attention gained by an item, namely *popularity*.

Note that the collected data would be complementary to the sale history based customer behavior analysis, even if the amount of detected pick-up actions is not proportion to the amount of sales. Indeed, disproportion between the popularity and sales of an item should be an important alert to the shopper or manufacture for adjusting their production plan or retailing strategy. In CBID, pick-up actions are detected by the movement of the tag attached to an item according to the analysis of signal changes.

2) ***Revealing explicit correlations****:* We say items have *explicit correlations* if they are rival or complementary. For example, a customer may compare a bottle of CocaCola and a bottle of Pepsi. As another example, a customer may pick up a cap and a jacket to decide if they match each other. Sales history analysis may reveal some of complementary items but can hardly discover rival items. The pick-up behaviors of explicit-correlated items are spatially and temporally close, e.g. a customer may pick up these items simultaneously (Figure 1(b)). The CBID system applies novel passive tag localization methods to reveal such spatial and temporal correlations of moving items.

3) ***Disclosing implicit correlations****:* We say items have *implicit correlations* if they share similar pick-up, moving, or purchase correlations. The most famous example is the tale of beer and diapers, which says that beer and diaper sales are explicitly correlated because young fathers who are sent to buy diapers would also buy beer for themselves. CBID uses tag trajectory monitoring and clustering to disclose these correlations by detecting and analyzing movement patterns of tags, as shown in Figure 1(c).

Among these three objectives, the first one focuses on the popularity of individual items. Meanwhile, the second and third ones focus on the items with correlations, explicitly or implicitly. Leveraging the results provided by CBID, retailers can obtain the information including which items are popular, which items simultaneously receive customer attentions, and which items are likely to be moved or selected by a same customer. This information helps retailers to determine which items should be displayed using more space and how items should be displayed.

B. Signal Characteristics

We briefly introduce the low level data collected and analyzed by CBID, $i.e.$, a number of signal characteristics of RFID reader and tag communication. CBID mainly use three signal characteristics, namely RF signal phase, received signal strength, and Doppler frequency shift.

1) ***RF signal phase****:* In RF signal, the phase is a periodic function with a period 2π radians. The measured phase φ follows

$$\varphi = 2\pi \cdot \left(\frac{d}{\lambda}\right) mod\,(2\pi) \tag{1}$$

where d is the distance from the transmitter to receiver and $\lambda = c/f$ is the wavelength of signal at frequency f (in Hz). In RFID systems, the phase model needs proper modifications because of two reasons. First, the tag replies to the reader in a backscatter way. The total distance for the backscattered signal traveling between the reader and tag is $2d$. Moreover, the reader's transmit circuits (φ_t) and receiver circuits (φ_r), the tag's reflection characteristic (φ_{tag}), will introduce additional phase rotation. Therefore, the phase of RF signal can be

(a) Discovering popular items (b) Revealing explicit correlations (c) Disclosing implicit correlations

Fig. 1. Three objectives of CBID.

modeled as:

$$\varphi = 2\pi \cdot (\frac{2d}{\lambda}) + \varphi_t + \varphi_r + \varphi_{tag} \tag{2}$$

*2) **Received signal strength**:* The Received Signal Strength (RSS) is a measurement on the power of a received radio signal. In RFID systems, RSS is one of the reader outputs, reflecting the power of received backscattered signal P_{Rx}. RSS can be measured in the unit of dbm and calculated as: $RSS = 10\lg(\frac{P_{Rx}}{1mW})$. According to the Friis Function [10], we also have a relationship between the transmitting and received power:

$$P_{Rx} = P_{Tx}T_bG_r^2G_t^2(\frac{\lambda}{4\pi d})^4 \tag{3}$$

where P_{Tx} is the transmitting power, T_b is the loss in the backscatter transmission, d is the distance between the reader's antenna and tag's antenna, and G_r and G_t are the gains of reader's antenna and tag's antenna respectively. We can then model RSS as:

$$RSS = 10\log(\frac{P_{Tx}}{1mW}T_bG_r^2G_t^2(\frac{\lambda}{4\pi d})^4) \tag{4}$$

*3) **Doppler Frequency Shift**:* The Doppler frequency shift (also known as the Doppler effect) reflects changes in frequency domain of a wave from its source to a moving receiver. Assuming the object moves at a velocity v and an angle of α from the receiver (reader antenna), then the Doppler frequency shift is modeled by:

$$\Delta f = \frac{2v}{\lambda} \cdot \cos(\alpha) \tag{5}$$

C. Improvement of Existing Reader API

In the implementation of CBID, we adopt an Impinj Speedway Revolution RFID reader to communicate with UHF passive tags. The Impinj newest software can report low-level data, such as the phase, RSS and Doppler shift, through an API compatible with the standard Low Level Reader Protocol (LLRP). However, from the observation of the collected data by the API, we find the measurement values are not accurate enough to satisfy the application requirements of CBID.

First, when the reader processes the received signal, it introduces some radians of ambiguity such that the reported phase can be either the true phase (φ) or the true phase plus radians ($\varphi + \pi$) [11]. Thus, we need to standardize the API outputs to unified values before further operations.

Second, many factors influence the reader's ability to obtain accurate Doppler estimates, such as the multiple effect in indoor environments, antenna switching, frequency hopping, and the Signal-to-Noise Ratio (SNR) of received signal. Targeting to these factors, there are several intuitive methods to increase the estimation accuracy.

Fixing on the maximum frequency. It is worth to note that phase estimates should only be compared on a single channel. And the doppler shift obtained from this API is measured indirectly on the phase. Hence, the channel should be fixed during experiments. Moreover, from Equation 5, we know larger frequency results in a more obvious doppler shift value.

Increasing EPC length. Longer packet durations ($i.e.$, longer measurement intervals) can increase the accuracy of estimating Doppler frequency shifts. One approach is to increase the Electronic Product Code (EPC) length. Following the commercial EPC C1G2 standard, the length of EPC code can be set to 96-bit at most [12]. We adopt this length in our implementation.

Adopting M8 reader inventory mode. As another approach to increase packet durations, the reader may use slower reader inventory mode ($i.e.$, Miller-8 mode) to slow down the communication rate.

Even with above improvements, the derived Doppler shift values, however, are still affected by noises. We measure Doppler shift values of 12 tags via the reader API and show the standard deviation in Figure 2. The points connected by blue lines indicate the standard deviations, which are very big. We propose a new solution to mitigate the impact from noises, which will be detailed in Section III. Shown by the red region in Figure 2, we find that the proposed phase-based doppler estimation can keep the standard deviation of Doppler value in very small values when tags are static.

D. System Overview

In the CBID system, passive tags are attached to commodities and a reader is deployed in charge of reading the tags via backscatter communication. The raw data collected by the CBID reader include the Electronic Product Code (EPC), signal phase, RSS, and timestamp. These data can further be derived to estimate Doppler shifts.

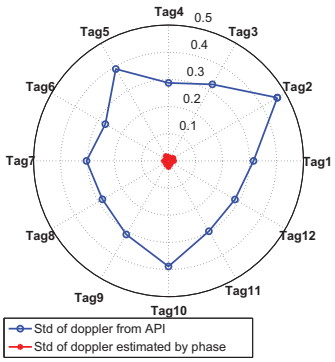

Fig. 2. Comparison of the standard deviation of doppler shift in static scenario. Our phase based doppler can keep the std of doppler value at nearly zero, while the std of doppler from API is rough.

Figure 3 illustrates the architecture of the CBID system. Based on the collected data, CBID first conducts signal processing tasks including phase pre-processing, Doppler shift calculation, and IMR calculation. It then uses the results of signal processing to achieve the three behavior identification objectives discussed in Section II-A.

In the following sections, we focus on describing how CBID performs behavior identification via discovery of popular items, explicit correlations, and implicit correlations.

III. Doppler-based Popular Item Discovery

Popular item discovery in CBID can be achieved by detecting and counting the pick-up events by customers. In this section, we propose an accurate and robust discovery algorithm of popular items discovery.

A. Doppler Shift Estimation

Doppler frequency shift reflects the relative velocity between a reader and tag. When a customer picks up a tagged item, the speed of item movement, $i.e.$, the velocity of the attached tag perpendicular to the reader antenna, can result in frequency shifts. However, a low-cost commercial RFID reader does not offer an accurate API for Doppler shifts.

To recognize the occurrence of Doppler shifts and improve accuracy, we investigate the insight of Doppler shifts in RFID communication in detail. We firstly consider a single tag moving radially to a reader antenna with velocity v. During this movement, the reader repeatedly identifies the tag by the received EPC packets. Assume that the reader receives two consecutive EPC packet P_i and P_{i+1}. Let t_i, t_{i+1} denote the time stamps of these packets arriving at the reader and ϕ_i, ϕ_{i+1} represent the corresponding signal phases. We can calculate the distance that the tag moves between two time stamps:

$$d = v \cdot (t_{i+1} - t_i) \tag{6}$$

The distance can also be presented by the corresponding phase shift of the signal collected between t_{i+1} and t_i. Note that the backscatter signal travels both the downlink and uplink, which makes the transmission distance equals to $2d$. Therefore, we obtain such an equation:

$$2v \cdot (t_{i+1} - t_i) = \lambda \cdot (\frac{\phi_{i+1} - \phi_i}{2\pi}) \tag{7}$$

From Equation 7, we can derive the expression of Doppler frequency:

$$f = \frac{v}{\lambda} = \frac{1}{4\pi} \cdot (\frac{\phi_{i+1} - \phi_i}{t_{i+1} - t_i}) \tag{8}$$

Equation 8 indicates that estimation of Doppler frequency depends on the phase change and time interval between two packets. If applying this estimation method, there should be two conditions.

- In the interval between two consecutive EPC packets, the tag should move less than half of a wavelength in the radial direction. Otherwise, the measurement on phase will suffer from under-sampling and the result cannot accurately reflect the phase shift. This condition can be easily satisfied using current commercial readers, e.g. Impinj R420.
- The received signal should be continuous. Some changes in reader transmitter, such as channel hopping, will cause inaccurate calculation on the distance in Equation 7. Therefore, we have to fix the transmitter configurations, including frequency channel and antenna selection, in steady state during signal measurement.

There is another challenge in data pre-processing stage before computing the Doppler frequency shift. It is known that the phase value is a periodic function, called the wrapped phase. In our system, one concern is that calculating the phase difference between two consecutive packets needs to consider all appropriate times of 2π, called phase unwrapping. We achieve this by using an One-Dimensional Phase Unwrapping method [13], which also requires continuous sampling as discussed in the first condition above.

To evaluate the effectiveness of our method, we conduct two experiments to compare the Doppler frequency values from Impinj API and our Doppler estimation scheme based on phase changes. Figure 4(a) shows the experiment results in a static scenario. We encode the tag ID with the longest bits-setting (96 bits) and encode the EPC packet with the Miller-8

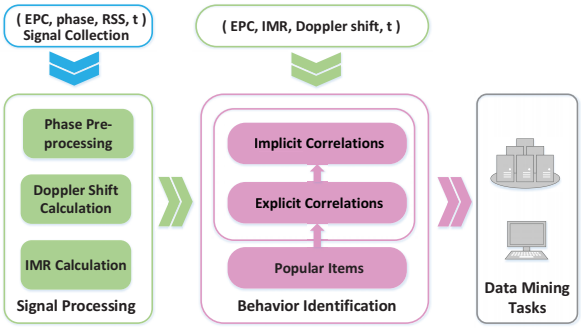

Fig. 3. System Architecture of CBID

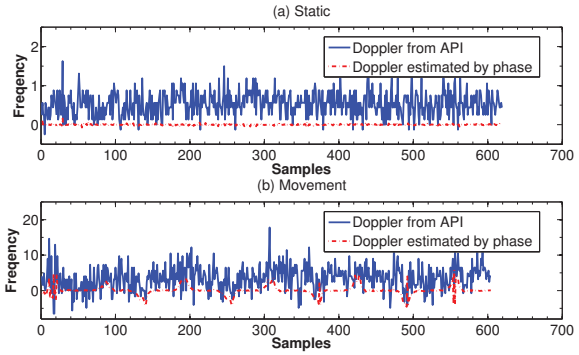

Fig. 4. Doppler frequency estimation by phase shift: (a) In the static scenario, Doppler readings from Impinj API change dramatically while the Doppler frequency estimated by our method is very stable. (b) In the movement scenario, the Doppler frequency estimated by our method can effectively distinguish tag movements, but that from Impinj API cannot.

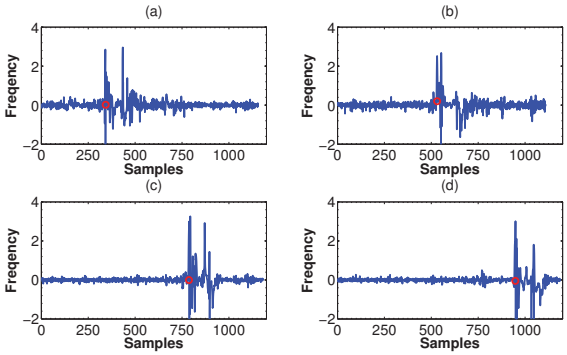

Fig. 5. Change point detection by adaptive CUSUM: The subfigures show the Doppler frequency changes of four continuous pick-up actions. The blue curve shows the estimated Doppler values and the red circles are the change points detected by adaptive CUSUM.

modulation. The frequency channel is also tuned to the largest one, which is 924.375 MHz for our reader. The blue line is the doppler frequency value collected from the Impinj API and the red dotted line is the estimation of doppler value using Equation 8. As visualized in Figure 4(a), the doppler value gained from Impinj API changes dramatically in the static scenario with a standard deviation of 0.3040, even if we apply the most favorable settings. On the other hand, results produced by the estimation scheme of CBID are much more stable, with a much smaller standard deviation 0.0167.

We also build up a movement scenario to simulate pick-up behaviors. At the very beginning, a volunteer holds a tagged item in front of the reader antenna. Then he moves his forearm repeatedly to make the item either towards or away from the antenna. In theory, the movement approaching the reader [14] will result in a positive peak in Doppler frequency and the opposite movement will lead to a negative peak value. When using our scheme, the experiment result is well compliant with the theory, as shown by the red curve in Figure 4(b). The periodic positive/negative peak changes clearly reflect customer's movements. However, the Doppler frequency values from Impinj API suffer from noise interference and cannot report the motions accurately.

B. Adaptive Doppler Peaks Detection

Accurate estimation of the Doppler frequency shift is the first step of detection of pick-up actions. Then the system should detect the peaks of Doppler frequency values quickly and precisely. Many existing algorithms have been proposed for frequency change detection or peak detection. However, they require to record measurement data and then apply analysis tools. In real deployment of the CBID system, keeping the values of Doppler frequency would be a overloaded task considering a huge amount of data will be generated by monitoring the movements of thousands of tags in very short time intervals. Therefore, we design an accurate magnitude threshold-based detection which drops the data not related to the Doppler change as much as possible. A challenge is that such a deterministic threshold does not exist because of two limitations in real deployment. 1) Tag diversity induces diverse noise levels across different tags, and 2) item locations diversity also raises different Doppler patterns. For the above reasons, we adopt an adaptive CUSUM algorithm [15] to track possible changes in Doppler values.

Let $d(t)$ denote the Doppler frequency value at time t and its probability density is denoted by p_θ, where θ is the distribution parameter. Assume that a change happens at time T, the probability density of Doppler frequency changes from p_x to p_y. Then we can use a logarithmic ratio to compare these two distributions:

$$l_y = log\frac{p_y(d(t))}{p_x(d(t))} \tag{9}$$

For the parameter x, it is easy to be obtained from the historical change record. But the parameter y, which is also called post-change distribution parameter, is unknown. It also varies during the detection process, leading more difficulty to predict.

To solve this problem, we define the change time T as:

$$T = inf\{t|\max\sum_{i=k}^{t} l_y(i) \geq h\}, 1 \leq k \leq t, \tag{10}$$

where h is a predefined value [16]. Given that the post-change distribution is unknown, the time T cannot be directly known from Equation 10. CBID then recursively applies the CUSUM method proposed in [15] to determine the range of parameter y. Based on the range of y, we can detect changes of the Doppler frequency more accurately.

We verify the feasibility of above solution via extensive experiments. We conduct experiments in three different scenarios described in Section VI-A3. Here we only show a small part of results about change point detection in Figure 5. Each of the subfigures 5(a)-(d) corresponds to a pick-up experiment. In such an experiment, a volunteer picks up a book from a shelve and puts it back. We record the signal phase and time stamp of every tag packet during this period. The blue curve represents the estimates of Doppler frequency calculated by Equation 8. By examining these estimates using the adaptive CUSUM algorithm, CBID detects a sudden change marked by

a red circle in each of the subfigures. Experimental results of four actions indicate that the algorithm works well in different scenarios. As a result, the CUSUM algorithm can successfully skip perturbations in signal caused by environmental noise and discover the real change point in Doppler frequency values.

IV. Location-based Explicit Correlation Discovery

We present our solution of explicit-correlated item discovery in this section. The main challenge is to connect items that are picked by a same person. However collected data are unable to report which items belong to whom. For the example of the scenario shown in Figure 1(b), two customers stand in front of a goods shelf. When three events of item pick-up are detected, our system should further figure out that two pick-up actions belongs to a same customer. It is generally the truth that when two items are holding by a same person, their positions should be close. Inspired by this, we form the problem of explicit correlation discovery as locating tagged items and deciding which tags are geographically close.

To locate close tags, an intuitive approach is to use the RSS of backscattered RF signal as the position fingerprint. Nevertheless, this method has some well-known drawbacks. First, it utilizes the Friis Equation that clarifies an RSS is inversely proportional to the biquadrate of the distance. The equation can only become valid with a strong assumption: the communication parties should be in a unobstructed free-space. In indoor environments, the multipath effect will yield severe influence to RSS measurement. Second, it is a huge workload to build an RSS map in advance. In addition, recent studies further show that such an RSS value strongly depends on the multipath profile [17]. Multipath profiling for localization, though being accurate, requires modifications on the reader hardware, e.g. adopting the technique of synthetic aperture radar. These modifications result in non-trivial customization overhead.

Thus, we propose to allow the reader to intentionally move its antenna and collect multiple RSS samples from a same tag at different antenna locations. CBID then uses multiple RSS from a same tag as a new metric for location. This method does not need any modification on existing RFID hardware and protocols.

A. Antenna Movement Model

Different from traditional RSS models where one tag location is assumed to be corresponded to a single RSS value, the proposed solution in CBID moves the reader antenna and collects multiple RSS samples for a tag. We first develop a simple antenna movement model to characterize the direction-distance relationship at different antenna locations. Based on that, CBID can retrieve the RSS information of tags and determine whether they are close or not. In this new model, there are two requirements.

- In order to improve the accuracy, it is better to avoid changing the dominance of direct path when antenna moves. So, the antenna should not move out of a range. We define an upper bound of this range as $\frac{Y}{5}$, where Y is the vertical distance between the antenna and tag (as shown in Figure 6).
- Inspired by Jakes Model [18], the signal within half wavelength are indistinguishable. Therefore the distance of antenna movement (r) has a lower bound $\frac{\lambda}{2}$.

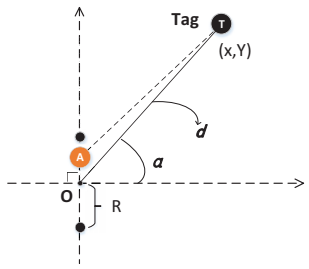

Fig. 6. Illustration of Antenna Movement Model

In summary, we have $\frac{Y}{5} \leq r \leq \frac{\lambda}{2}$. To meet these conditions, we prefer to simply move an antenna back and forth in our implementation, termed as shuttle antenna. Figure 6 illustrates an example of the antenna movement model, where O is the origin location of antenna, T is a static tag at position (x, Y) with distance d from O, and the direction from O to T is in the angle α. A is the shuttle antenna. The position vector of tag T is :

$$\overrightarrow{OT} = (d \cdot \cos\alpha, d \cdot \sin\alpha) = (x, Y) \tag{11}$$

Suppose that A moves along the vertical axis within a maximum range R. The displacement of A periodically changes with t within the range $(-R, R)$. We take a sine function to simulate this displacement for simplicity. Therefore, the position vector of A can be represented as:

$$\overrightarrow{OA} = (0, R \cdot \sin t) \tag{12}$$

The distance vector from the antenna to tag is $\overline{AT}$:

$$\begin{aligned} \overrightarrow{AT} = \overrightarrow{OT} - \overrightarrow{OA} &= (x, Y) - (0, R \cdot \sin t) \\ &= (x, Y - R \cdot \sin t) \end{aligned} \tag{13}$$

B. Integration of Multi-RSS

We also propose to use a new metric, called Integration of Multi-RSS (IMR), as the fingerprint of a tag's location. By moving the reader antenna, CBID obtains a set of RSS values for a fixed tag ($i.e.$, a fixed location) when the antenna moves. The RSS value varies because $\overline{AT}$ changes. Let $M = \frac{P_{Tx}}{1mW} \cdot {G_r}^2 {G_t}^2 T_b (\frac{\lambda}{4\pi})^4$. According to Equation 4, at time t, the RSS received from the tag can be represented as:

$$\begin{aligned} RSS(t) &= 10\lg(M \cdot \frac{1}{|AT|^4}) \\ &= 10\lg(M \cdot (\frac{1}{\sqrt{x^2 + (Y - R\sin t)}})^4) \\ &= 10\lg(M \cdot (\frac{1}{x^2 + (Y - R\sin t)})^2) \end{aligned} \tag{14}$$

Let P_{Tx} be transmit power of reader, which is set to $32dbm$. G_r is $8dbi$ for our reader antenna Laird A9028R30NF. G_t is $2dbi$, which is the typical gain for real dipole-like tag antenna. T_b is $\frac{1}{3}$ [10] here for backscatter transmission loss. Y can be measured through real deployment and in our experiment, we put the shuttle antenna $1m$ away from the tags. Then, the only unknown parameters in Equation 14 are the tag's horizontal axis value x and the time t. The IMR metric is used to reflect t and x, and thereby fingerprint the tag's location.

The CBID reader collects the RSS values of a tag in a complete antenna movement cycle. The multiple RSS values together provide the IMR fingerprint of the tag, $\int_0^{2\pi} RSS(t)dt$:

$$\begin{aligned}
&\int_0^{2\pi} RSS(t)dt \\
&\quad = \int_0^{2\pi} (10\lg(M \cdot (\frac{1}{x^2 + (Y - R\sin t)})^2))dt \\
&\quad = \int_0^{2\pi} 10\lg M dt - \int_0^{2\pi} (20\lg(x^2 + (Y - R\sin t)))dt \\
&\quad = 10\int_0^{2\pi} \lg M dt - 20\int_0^{2\pi} \lg(x^2 + (Y - R\sin t))dt
\end{aligned} \tag{15}$$

Replacing $\sin t$ with θ in Equation 15, we have

$$\begin{aligned}
&\int RSS(\theta)d\theta \\
&\quad = 10\int_0^{2\pi} \lg M dt - 20\int_0^{2\pi} \frac{\lg(x^2 + (Y - R\sin t)) \cdot \cos t dt}{\cos t} \\
&\quad = 10\int_{-1}^{1} \lg M d\theta - (20\int_0^{1} \frac{\lg(x^2 + (Y - R\theta))d\theta}{\sqrt{1-\theta^2}} \\
&\quad + 20\int_{-1}^{1} \frac{\lg(x^2 + (Y - R\theta))d\theta}{\sqrt{1-\theta^2}} \\
&\quad + 20\int_{-1}^{0} \frac{\lg(x^2 + (Y - R\theta))d\theta}{\sqrt{1-\theta^2}})
\end{aligned} \tag{16}$$

Given different x values in Equation 16, we can achieve the relationship between the tag locations and the proposed fingerprint IMR, which is demonstrated in Figure 7. We can see that when a tag's vertical distance Y to the antenna is constant, its IMR value is inversely proportional to the tag's horizontal distance x.

The IMR metric is better than those used by traditional RSS methods for tag localization with the following reasons. Let S be the signal vector received from a given tag. S can be considered as the sum of a multi-path signal *MPS* and a noise signal N. Thus, we have the expression $S = MPS + N$. Normally, we can assume that the noise signal follows a typical gaussian distribution with a mathematical expectation of 0. Hence the integral value of N should tend to 0. On the other hand, the multi-path effect may cause RSS changes. In some positions and angles the RSS may be strengthened, while in other cases, the RSS may be weakened. In our implementation, we adopt the shuttle antenna pattern and collect a set of RSS values for each tag's position. Multiple sampling of a tag can help the system to neutralize the multi-path effect. Therefore, IMR-based localization has a better performance than single-RSS based approaches.

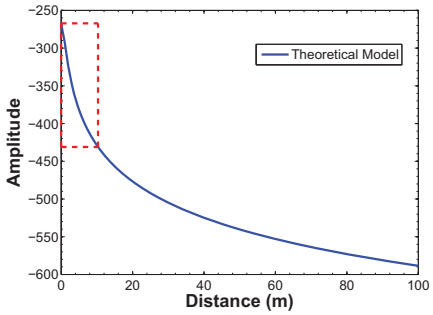

Fig. 7. The IMR values of different tag positions from our theoretical model, given the same vertical distance. The red dotted box marked the practical reader range in $0 \sim 10$ meters.

V. Movement Pattern Based Implicit Correlation Discovery

Based on Section III, the CBID system knows which items are picked up by customers. Furthermore, we expect to find out the reason behind. For example, a customer who has put onions and tomatoes into the shopping cart may also buy burgers. This correlation can be expressed as $Pre\{Onion, Tomato\} \Rightarrow Pn\{Burger\}$. $Pre\{\}$ represents that a customer picked the item previously, while $Pn\{\}$ represents that the customer is likely to pick the item in future. Previously picked items may be in hand or in a shopping cart, within a short range in either way. Identifying $Pre\{\}$ and $Pn\{\}$ items helps the system to connect items with implicit correlations.

A. Problem Formulation

When a customer chooses $Pn\{\}$ items and leaves the shopping area together with his/her $Pre\{\}$ items, the reader can easily detect the movement of these items. Hence if only one customer stands in the area, the correlated items are relatively easy to detect. However, real situations are much more complicated. Considering two or more customers $(C_1, C_2, ..., C_n)$ who are shopping in front of a shelf and they all have their wished items. Some of them may have picked some items and leaved this area almost at the same time. We denote all tags belonging to these customers are *near-context* tags for this area. The near-context tags are actually identified in one area of interests and their time stamps of residence differ slightly within certain time tolerance. In our experiments, we set the time tolerance as 0.5 second.

Then the problem is formulated as, giving all the data of near-context tags, for each $Pn_i\{\}$ item how to discover the previous items set $Pre_i\{\}$ which belongs to the same customer C_i.

One intuitive solution to this problem is to record each tag's Doppler frequency value and monitor its movement trajectory. For the items in a same shopping cart, they will move together

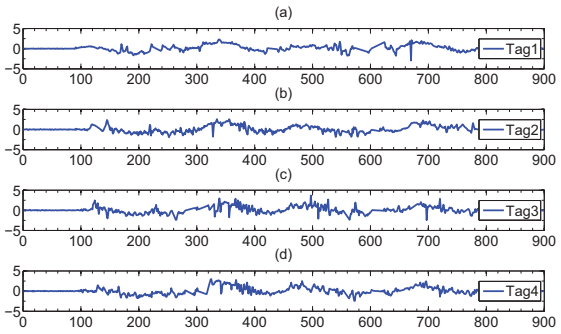

Fig. 8. Doppler data of implicit-correlation experiment: Subfigure (a)-(d) demonstrate 4 tags' doppler data after segment-based interpolation. Tag1 belongs to volunteer A and the other 3 belong to volunteer B.

and share a similar movement pattern. The traces of all near-context tags can be clustered to different customers. However, such a solution encounters two challenges in a real RFID system.

- Irregular sampling period: In an UHF RFID system, identifying tags will experience a collision-arbitration process, by which different tags are identified in different time slots. This means the sampling time for different tags will not be the same. In addition, several other factors, such as signal attenuation due to tag movement, will also lead different sampling times to different tags. This problem makes the sample density varies over time for each tag and then ruins the accuracy of clustering.
- Unknown number of customers: As the number of customers is unknown for the system, exhaustive search for the best clustering result is an NP hard problem. Therefore, an effective clustering algorithm with rapid convergence is required.

B. Segment-based Interpolation

To overcome the first challenge, we implement a segment-based interpolation approach which makes all raw data have the same number of samples of different tags. We set the time length of one segment as $T_{seg} = 1s$ and find the minimal time stamp (T_{min}) and maximal time stamp (T_{max}) of all data reported from near-context tags.

Then the whole time period is partitioned into N segments, where $N = \lceil (T_{max} - T_{min})/T_{seg} \rceil$. In each segment, CBID applies the Linear Interpolation method to fit the Doppler curves. The advantage of this method is that we can reduce the interpolated error. In addition, considering each segment of data is indeed one observation, this method will increase the amount of data used for the clustering algorithm presented in the next subsection.

C. Iterative Clustering Algorithm with Cosine Similarity

In this subsection, we present an iterative clustering approach to organize tags in different groups, which utilizes cosine similarity measurements.

To clearly explain the goal of this algorithm, we use one group of experiment data to serve as an example. Figure 8 shows tags' Doppler frequency data processed by the segment-based interpolation. In this set of experiments, two volunteers emulate a shopping procedure and each of them has a shopping cart. Their trajectories are random. Volunteer A has only one item which is associated with Tag1. The other three items (with Tag2 Tag3 and Tag4, respectively) are all in volunteer B's shopping cart. In order to extract implicit correlations of the items, we have to cluster the four tags.

As described in Section V-B, we divide the Doppler data into N segments. Each segment of data is considered as a vector. We implement the cosine calculation to measure the similarity between two vector observations within the same time period. Supposing there are M near-context tags. The similarity metric $S^i_{j,k}$ for two segments F^i_j, F^i_k can be expressed as :

$$S^i_{j,k} = \frac{F^i_j \cdot F^i_k}{\left\|F^i_j\right\| \left\|F^i_k\right\|}, 1 \le i \le N, 1 \le j,k \le M \tag{17}$$

where i denotes the ith segment of Doppler data and j,k are tags' identifiers. The similarity ranges from -1 to 1, where -1 means completely different and 1 means exactly the same.

For each time period i, $\binom{M}{2}$ times of comparisons should be conducted. Considering all the time periods, the size of the result matrix is $\binom{M}{2} \times N$:

$$\begin{bmatrix} S^1_{2,1} & S^2_{2,1} & \cdots & S^N_{2,1} \\ S^1_{3,1} & S^2_{3,1} & \cdots & S^N_{3,1} \\ \vdots & & \cdots & \vdots \\ S^1_{M,M-1} & S^2_{M,M-1} & \cdots & S^N_{M,M-1} \end{bmatrix} \tag{18}$$

The rows of the above matrix show all segments' similarity values between two segments of Doppler data. Therefore, the mean value of each row (*MS*) can reflect the average similarity of the Doppler data under comparison. Then we get the similarity vector:

$$R^t = [MS^t_{2,1}, MS^t_{3,1}, \cdots, MS^t_{M,M-1}] \tag{19}$$

where t indicates the tth iteration in our clustering algorithm. Giving the vector R^t, we can calculate a similarity threshold $Thre^t$ as:

$$Thre^t = mean(R^t) + \alpha * std(R^t) \tag{20}$$

where α is a constant value.

We continue to use the example of Figure 8 to explain the effectiveness of our algorithm. At first, each tag is considered as one individual cluster. According to Equations 17, 18, 20, we can calculate the first similarity vector R^1 based on the measured data of the four tags. The results are shown in Figure 9. Each number in this figure means the average similarity between two tags. The threshold of the first iteration is 0.47, if $\alpha = 1$. We pick similarity values which are greater than the threshold: $MS^1_{3,4}$ in our example and put the two corresponding tags into one cluster. Hence Tag3 and Tag4 are clustered in the first iteration. The mean similarity R^2 and the threshold $Thre^2$ should be re-calculated in next iteration. When there is no similarity value is greater than the threshold,

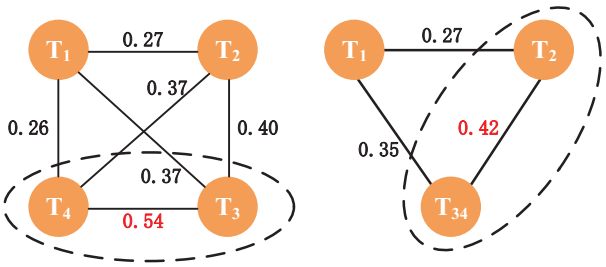

Fig. 9. An example of iterative clustering algorithm.

or only one cluster left in the end, the iterative algorithm is terminated.

VI. Implementation and Evaluation

In this section, we present the prototype implementation of CBID and evaluate its performance by conducting comprehensive experiments.

A. Implementation

*1) **Hardware**:* In the implementation of CBID, we adopt a Commercial-Off-The-Shelf (COTS) Impinj reader, *i.e.*, Impinj R420. The reader works at the frequency of 924.375 MHz, which is the maximum frequency available for our region. Two directional antennas (Laird A9028R30NF with a gain of 8dbi) were used in our experiments. One antenna is mounted on the ceiling of the lab. The shuttle antenna is mounted on a sliding rack. The sliding rack consists of a motor for moving the antenna forth and back. For adjusting the moving velocity and direction, a circuit unit control the rotate speed of motor changed in a sine function pattern. We use two types of COTS UHF passive tags from two mainstream manufactures, Alien and Impinj.

*2) **Software**:* We have implemented the software in charge of data collection and analysis on a high performance computer. The software is integrated with the Octane SDK, an extension of the LLRP Toolkit, which supports the report of low-level data including signal phase, RSS, and Doppler shift.

*3) **Experiment Scenarios**:* Referring to common display modes in B&M stores, our experiments cover the following typical scenarios.

- *Line mode (clothes):* Many commodities are displayed on a shelf in line, we implement this scenario in our lab by hanging clothes on a rack, as shown in Figure 10(a).
- *Horizontal mode (glasses):* This mode is familiar with the counter in shopping malls. The commodities are displayed in a horizontal plane. We put a number of glasses on a table to simulate this scenario. Figure 10(b) shows the experiment deployment.
- *Vertical mode (books):* This mode is the most common display scenario in supermarkets and libraries. We have implemented this scenario in a university library and tagged the books on shelf, as shown in Figure 10(c).

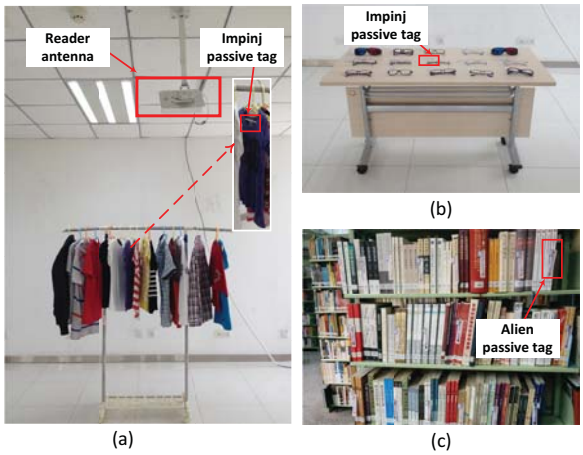

Fig. 10. Three scenarios in our implementation. (a) Line mode using clothes. (b) Horizontal mode using glasses. (c) Vertical mode using books.

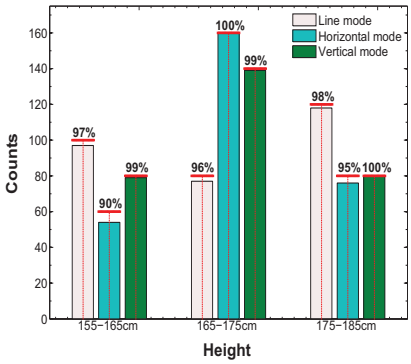

Fig. 11. Accuracy of pick-up detection for different human height ranges

B. Accuracy of Pick-up Action Recognition

We first focus on the pick-up action recognition for popular items discovery and evaluate its accuracy across all three scenarios. The experiments were conducted inside our lab with the reader antenna mounting on the ceiling. We invited 25 volunteers to participate the experiments. Their heights vary from 155 to 185 cm. We run 300 experiments for each scenario introduced in Section VI-A3. In each experiment, 15 volunteers were asked to pick 5 items arbitrarily among 20 tagged items.

Figure 11 demonstrates the counts of picking behaviors detected in three scenarios as well as the comparison to the ground truth. The body heights are classified into three groups, 155 - 165 cm, 165 - 175 cm, and 175 - 185 cm. In this figure, the bars represent the detected counts, while the lines represent the ground truth. We find that there is very little impact of the heights to accuracy. Even in the worst case, *i.e.*, the case of horizontal mode with 155 - 165 cm heights, the accuracy still reaches 90%. These results show that our method is robust among different scenarios and different human heights.

TABLE I
ACCURACY OF PICK-UP DETECTION IN THREE SCENARIOS

Category	Line	Horizontal	Vertical	Overall
Accuracy (%)	97.33	96.67	99.33	97.78

In the results of total 900 experiments, the overall accuracy reaches up to 97.78%. The precision of three scenarios are compared in Table I. We find that the vertical mode shows the highest accuracy over 99% while the horizontal mode has the lowest accuracy among three scenarios.

C. Accuracy of Explicit Correlation Discovery

We evaluate the accuracy of explicit correlation discovery described in Section IV by identifying tagged items that are picked by a same customer. We conduct this set of experiments using the line mode scenario, marking 5 locations on a rack, 40 cm apart for adjacent locations. Based on life experience, we believe 40 cm is a reasonable distance between two persons. If two tags are 40 cm or more apart after being picked up, we consider they belong to different customers. Otherwise, they belong to a same customer. In addition, the shuttle antenna used in this set of experiments is on one side of the clothes rack, and its moving direction is perpendicular to the cross rod of the rack. We take the difference of two tags' IMR values (ΔI) as the metric to identify the distance between tags. The threshold (θ) is used to distinguish whether the distance is longer than 40 cm. We adopt Equal Error Rate (EER) method to decide the threshold (θ).

1) ***Selection of threshold*** *:* We determine θ as follows. We separate the experiments into two categories. ***Case 1: 1-Person 2-Item:*** We put two tags within the safe distance, and then change their positions. In this case, we use the distance equal to 10 cm to emulate the situation of two tags in one hand and use distance equal to 20 cm to emulate the situation of two tags in two hands of a same person. Thus, we have $\binom{5}{1} * \binom{2}{1} = 10$ groups of experiments. ***Case 2: 2-Persons 2-Item:*** We let tag A always in the front of tag B, then polling in all 5 positions. Thus we have $\binom{4}{1} + \binom{3}{1} + \binom{2}{1} + \binom{1}{1} = 10$ groups of tests. We repeat every test 5 times, resulting a total number of 100 experiments. We calculate ΔI for every of them.

We try different values of the threshold θ to compute the rate of falsely rejected and falsely accepted cases. ΔI from Case 1 that is above θ indicates a case of false reject, and ΔI from Case 2 that is below θ indicates a case of false accept. Based on the results we compute the False Reject Rate (FRR) and False Accept Rate (FAR). The Equal Error Rate (EER) is a value where FRR equals to FAR. EER is a common metric to measure performance of a recognition system. When θ is set to the EER, the system can achieve the lowest sum of FRR and FAR. As shown in Figure 12, when we calculate ΔI using RSS data from 4 integration cycles, the EER is 0.15 and θ is 418.

When CBID serves as a data provider for backend data mining servers, it may try to provide less dirty data. In this case, CBID prefers to reduce the FAR, while sacrifices the FRR. For example, θ can be as 359, and then the FAR is 10% and FRR is 18%.

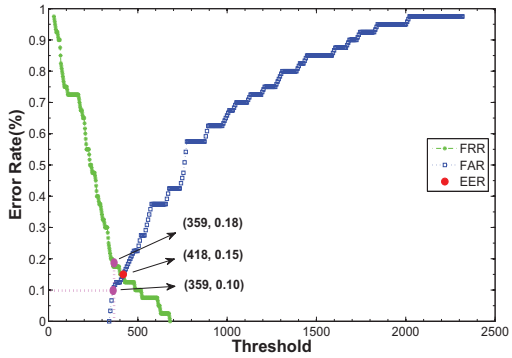

Fig. 12. Selection of θ according to FRR and FAR when the integration cycle is 4.

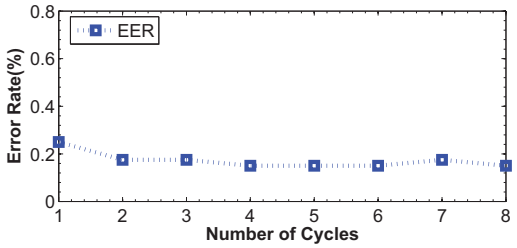

Fig. 13. EER versus number of integration cycles

2) ***Accuracy Versus Number of Cycles****:* To investigate the relation between accuracy and the number of integration cycles, we calculate ΔI of different testing cases by varying the number of cycles. Figure 13 shows that EER reduces gradually while the number of cycles grows. When the number of cycles is 4, EER is 15%, which means the overall accuracy achieves 85%. In our experiment, we set the default number of cycles as 4 and the shuttle antenna's cycle duration as 0.8s. Hence, 4 cycles might be equivalent to $3.2s$. It is a reasonable time duration in practice for collecting the RSS data needed by the system.

D. Accuracy of Implicit Correlation Discovery

In this section, we analyze the accuracy of the clustering algorithm proposed in Section V, which aims at disclosing the implicit correlations. Experiments are conducted in a supermarket and tags are attached with different items. Experiments in this section focus on three questions. First, when multiple items belong to a same customer, can the algorithm successfully detect their similar trajectories? Second, when the number of customers increases, can the algorithm still yield good performance? Third, how long movement duration is enough for the algorithm to accurately cluster items? We adopt the FAR to evaluate clustering accuracy.

1) ***Performance of clustering****:* We conduct two types of experiments to answer the first and second questions. In the

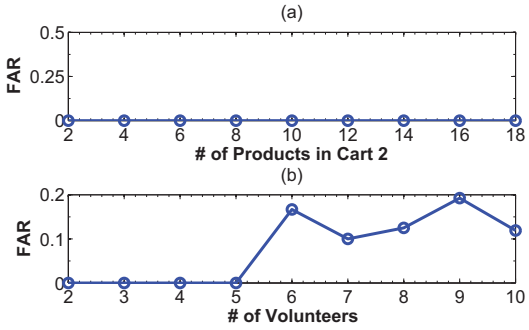

Fig. 14. Accuracy of tag clustering: (a) Multi-item experiment. (b) Multi-customer experiment

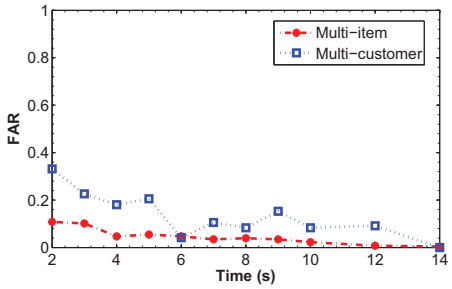

Fig. 15. Different movement time durations versus clustering accuracy

first set of experiments, two volunteers take shopping carts with them. Volunteer A keeps two items in his cart during the whole experiment procedure. The other volunteer B puts new items into his cart constantly. When each time B picks a new item, we implement the cluster algorithm to distinguish different trajectories. We vary the number of items selected by B from 2 to 18. Each set of experiments is repeated by five times. As shown in Figure 14(a), our algorithm can achieve zero false acceptance in all groups of experiments. On the other hand, the average FRR of this experiment is 0.13, which is higher than the FAR, but still within an acceptable error tolerance for our sensing scenario.

In the second set of experiments, we gradually increase the number of volunteers in the area. Each volunteer walk randomly with 2 items in hand. The maximum number of volunteers is 10 and we conduct 10 experiments for each setting. Figure 14 (b) shows the FAR versus different number of customers. The results show that when there are less than 5 customers in the area, no misclassified product is grouped into the high-profile cluster. With the number of customers growing, the FAR increase from 0.1 to 0.2.

These two group of experiments demonstrate that CBID performs well in both multi-item and multi-customer scenarios.

*2) **Evaluation of Time Efficiency**:* Time duration in above experiments is set in a fixed length, 30 seconds. However, in real shopping environment, customers usually leave one shelf at different speeds and it may not guarantee a 30-second time duration for data collection. Therefore, we have to evaluate the system performance with different time durations. To reuse data from the experiments above, we intercept different movement durations to serve as input signal for the cluster algorithm. As shown from Figure 15, the FAR is relatively high when the time duration is extremely short, especially for multi-customer cases. If the time duration is longer than four seconds, the input data are enough to yield accurate clustering.

VII. Related Works

Customer behavior analysis is important to current retail business. In this section, we briefly introduce the related works from two aspects, customer behavior identification, RF based localization, tracking, and motion detection.

A. User Behavior Collection

Sales history is an important source for customer behavior analysis. However it only reflects the items purchased by customers and misses other customer behaviors [19]. Compared to in-store shopping, online shopping [20], [21] is easy to complete this task. Online shoppers' behaviors, such as clicks, price comparisons, and search records, etc., can be captured by the Web.

For Brick and Mortar (B&M) stores, capturing the customer behaviors is extremely difficult. Most existing approaches depend on specific devices for monitoring and capturing user behaviors. R. L. Angell [21] deployed sensors to collect multi-dimensional environment data, such as location, temperature, humidity, lighting, etc. Deploying the data collection device in shopping cart was also proposed [22]. T. Kanda et al. deployed a sensor network with many six laser range finders in a shopping arcade [23]. The purpose of their work is to track and cluster customer trajectories to locate potential consumers. These solutions all rely on expensive devices for monitoring purposes.

B. RF based Localization, Tracking, and Motion Detection

RF based sytems, including WSN [24], RFID [3][17] and WiFi [25][26][27], have been extensively studied for localization, tracking, and motion detection. RFID tags mainly fall into two categories, active and passive tags. Active tags have on-board batteries as the power source such that they have more powerful computing capacity and storage than passive tags. Most active tag based localization approaches depend on the disturbance from people on RF signal [3]. Some of them can achieve device-free localization [28]. Due to the high cost of active tags, researchers proposed to use a hybrid RFID system [4], including some active tags as the location anchors and the majority passive tags as the disturbance detectors, for localization. On the other hand, since passive tags are extremely weak in computer power compared to active tags, they are usually used for identification only. Recently, passive tag localization and tracking is also investigated. Utilizing multipath effect, passive RFID tags can support accurate location reference [17]. Besides signal strength, some other

features, such as the phase [5], mutual interference [29], and the angel between the antennas of reader and tag [30], are also used to improve the localization accuracy. It is worth to note that antenna movements, which has been used for outdoor localization [31], has become a promising way to locate passive tags with high accuracy [17].

WiFi signal is another major media used for motion-detection and localization. RADAR is designed for indoor localization and tracking using the Received Signal Strength (RSS) [32]. EZ [33] enables the location estimation on unknown positions without the need of pre-deployment. WiTrack [34] implements a system which tracks the person's 3D motion based on the radio signal reflected off his body. WiSee [14] enables whole-home gesture recognition using WiFi Doppler shift.

VIII. Conclusion

In this paper, we present the design, implementation, and evaluation of the CBID system. The CBID system leverages physical-layer information retrieved from the communication signal of passive tags to detect and track their movements. Correlations among tagged items can then be inferred. The protocols of CBID are simple and have no need of hardware modifications on off-the-shelf RFID devices. Results from our implementation and deployment show that CBID can achieve fast and accurate customer behavior identification in various circumstances. Our future work includes modeling of more complicated customer behavior and improving identification accuracy and reliability.

Acknowledgment

This work is partially supported by the National Natural Science Foundation of China (NSFC) under Grant No. 61325013, 61033015, 61373175, and 61402359, Specialized Research Fund for the Doctoral Program of Higher Education under Grant No. 20130201120016, and the Fundamental Research Funds for the Central Universities of China under Project No. 2012jdgz02 (Xi'an Jiaotong University).

References

[1] B. Pradel, S. Sean, J. Delporte, S. Guérif, C. Rouveirol, N. Usunier, F. Fogelman-Soulié, and F. Dufau-Joel, "A Case Study in a Recommender System Based on Purchase Data," in *Proceedings of ACM KDD*, 2011.

[2] W. Ltd., "The Data Storm: Retail and the Big Data Revolution," An Economist Intelligence Unit Report, Tech. Rep., 2014.

[3] L. M. Ni, Y. Liu, Y. C. Lau, and A. P. Patil, "LANDMARC: Indoor Location Sensing using Active RFID," *Wireless networks*, vol. 10, no. 6, pp. 701–710, 2004.

[4] D. Zhang, J. Zhou, M. Guo, J. Cao, and T. Li, "TASA: Tag-free Activity Sensing using RFID Tag Arrays," *IEEE Transactions on Parallel and Distributed Systems*, vol. 22, no. 4, pp. 558–570, 2011.

[5] T. Liu, L. Yang, Q. Lin, Y. Guo, and Y. Liu, "Anchor-free Backscatter Positioning for RFID Tags with High Accuracy," in *Proceedings of IEEE INFOCOM*, 2014.

[6] C. Qian, Y. Liu, H. Ngan, and L. M. Ni, "ASAP: Scalable Identification and Counting for Contactless RFID Systems," in *Proceedings of IEEE ICDCS*, 2010.

[7] C. Qian, H. Ngan, Y. Liu, and L. M. Ni, "Cardinality Estimation for Large-scale RFID Systems," *Parallel and Distributed Systems, IEEE Transactions on*, vol. 22, no. 9, pp. 1441–1454, 2011.

[8] D. Ma, C. Qian, W. Li, J. Han, and J. Zhao, "GenePrint: Generic and Accurate Physical-layer Identification for UHF RFID Tags," in *Proceedings of IEEE ICNP*, 2013.

[9] IDTechEx, "RFID Forecasts, Players & Opportunities 2014-2024," http://www.idtechex.com/search/?query=RFID, 2014.

[10] D. M. Dobkin, *The RF in RFID - Passive UHF RFID in Practice*. Elsevier, 2008.

[11] Impinj, *Speedway Revolution Reader Application Note - Low Level User Data Support*. Technical Report, 2013.

[12] EPCglobal, *Specification for RFID Air Interface EPC Radio-Frequency Identity Protocols Class-1 Generation-2 UHF RFID Protocol for Communications at 860 MHz-960 MHz*, 2008.

[13] K. Itoh, "Analysis of the Phase Unwrapping Algorithm," *Applied Optics*, vol. 21, no. 14, pp. 2470–2470, 1982.

[14] Q. Pu, S. Gupta, S. Gollakota, and S. Patel, "Whole-home Gesture Recognition using Wireless Signals," in *Proceedings of ACM MobiCom*, 2013.

[15] C. Li, H. Dai, and H. Li, "Adaptive Quickest Change Detection with Unknown Parameter," in *Proceedings of IEEE ICASSP*, 2009.

[16] E. Page, "Continuous Inspection Schemes," *Biometrika*, pp. 100–115, 1954.

[17] J. Wang and D. Katabi, "Dude, Where's my Card?: RFID Positioning that Works with Multipath and Non-line of Sight," in *Proceedings of ACM SIGCOMM*, 2013.

[18] D. Tse, *Fundamentals of Wireless Communication*. Cambridge university press, 2005.

[19] A. Ainslie and P. E. Rossi, "Similarities in Choice Behavior across Product Categories," *Marketing Science*, vol. 17, no. 2, pp. 91–106, 1998.

[20] J. Wang and Y. Zhang, "Opportunity Model for e-Commerce Recommendation: Right Product; Right Time," in *Proceedings of ACM SIGIR*, 2013.

[21] R. L. Angell and J. R. Kraemer, "Method and Apparatus for Identifying Unexpected Behavior of a Bustomer in a Retail Environment Using Detected Location Data, Temperature, Humidity, Lighting Conditions, Music, and Odors," Mar. 15 2011, US Patent 7,908,237.

[22] T. P. O'hagan and D. B. Van Horn, "Shopping Cart Mounted Portable Data Collection Device with Tethered Dataform Reader," Oct. 13 1998, US Patent 5,821,512.

[23] T. Kanda, D. F. Glas, M. Shiomi, H. Ishiguro, and N. Hagita, "Who Will be the Customer?: a Social Robot that Anticipates People's Behavior from Their Trajectories," in *Proceedings of ACM Ubicomp*, 2008.

[24] Z. Yang and Y. Liu, "Quality of Trilateration: Confidence-based Iterative Localization," *IEEE Transactions on Parallel and Distributed Systems*, vol. 21, no. 5, pp. 631–640, 2010.

[25] K. Wu, J. Xiao, Y. Yi, D. Chen, X. Luo, and L. M. Ni, "CSI-based Indoor Localization," *IEEE Transactions on Parallel and Distributed Systems*, vol. 24, no. 7, pp. 1300–1309, 2013.

[26] B. Li, P. Yang, J. Wang, Q. Wu, S.-J. Tang, X.-Y. Li, and Y. Liu, "Optimal Frequency-temporal Opportunity Exploitation for Multichannel Ad Hoc Networks," *IEEE Transactions on Parallel and Distributed Systems*, vol. 23, no. 12, pp. 2289–2302, 2012.

[27] W. Xi, J. Zhao, X.-Y. Li, K. Zhao, S. Tang, X. Liu, and Z. Jiang, "Electronic Frog Eye: Counting Crowd Using WiFi," in *Proceedings of IEEE INFOCOM*, 2014.

[28] Y. Zhao, Y. Liu, and L. M. Ni, "VIRE: Active RFID-based Localization using Virtual Reference Elimination," in *Proceedings of IEEE ICPP*, 2007.

[29] J. Han, C. Qian, W. Xing, D. Ma, J. Zhao, P. Zhang, W. Xi, and J. Zhiping, "Twins: Device-free Object Tracking using Passive Tags," in *Proceedings of IEEE INFOCOM*, 2014.

[30] S. Azzouzi, M. Cremer, U. Dettmar, T. Knie, and R. Kronberger, "Improved AoA Based Localization of UHF RFID Tags Using Spatial Diversity," in *Proceedings of IEEE RFID-TA*, 2011.

[31] Z. Zhang, X. Zhou, W. Zhang, Y. Zhang, G. Wang, B. Y. Zhao, and H. Zheng, "I am the Antenna: Accurate Outdoor AP Location using Smartphones," in *Proceedings of ACM MobiCom*, 2011.

[32] P. Bahl and V. N. Padmanabhan, "RADAR: An In-building RF-based User Location and Tracking System," in *Proceedings of IEEE INFOCOM*, 2000.

[33] K. Chintalapudi, A. Padmanabha Iyer, and V. N. Padmanabhan, "Indoor Localization without the Pain," in *Proceedings of ACM MobiCom*, 2010.

[34] F. Adib, Z. Kabelac, D. Katabi, and R. C. Miller, "3D Tracking via Body Radio Reflections," in *Proceedings of USENIX NSDI*, 2014.